Changes in a Gel's Electrical Properties Due to Exposure to Air

by

Amy Nicole Englehart

Submitted to the Department of Electrical Engineering and Computer Science
in partial fulfillment of the requirements for the degree of

Master of Science in Electrical Engineering and Computer Science

at the

MASSACHUSETTS INSTITUTE OF TECHNOLOGY

June 2002

Author .....
Department of Electrical Engineering and Computer Science
February 2, 2002

Certified by .....
Dennis M. Freeman
Associate Professor
Thesis Supervisor

Accepted by .....
Arthur C. Smith
Chairman, Department Committee on Graduate Students

Changes in a Gel's Electrical Properties Due to Exposure to Air

by

Amy Nicole Englehart

Submitted to the Department of Electrical Engineering and Computer Science
on February 2, 2002, in partial fulfillment of the
requirements for the degree of
Master of Science in Electrical Engineering and Computer Science

Abstract

A two-bath technique has recently been developed to measure the potential of the tectorial membrane, a gelatinous structure in the inner ear. The two-bath technique gives more stable measurements than previous techniques. However, results for the two-bath technique suggest physiologically unrealistic large concentrations of fixed charge in the tectorial membrane. One hypothesis to account for the unrealistically large concentration of fixed charge is that because the two-bath technique causes part of the TM to be exposed to air, it shrinks. Because of its smaller volume, its concentration of fixed charge would increase. For this thesis, artificial gels were fabricated and used to test this air-exposure hypothesis. The gel's potential was measured with the two-bath technique and also with a variation of the two-bath technique in which the gel was not exposed to air. In the two-bath experiments where the gel was exposed to air, it shrunk and fixed charge concentration estimates of the gel were larger than the fixed charge concentration estimates of the gel from the two-bath experiments when the gel was not exposed to air.

Thesis Supervisor: Dennis M. Freeman
Title: Associate Professor

Acknowledgments

Working with Denny has been a joy. I have learned an enormous amount about objective, meticulous and creative scientific research. His passion for understanding our world and openly sharing what he understands will always stay with me.

I'm so grateful to have been in a lab with so many kind people. A.J. has helped me immeasurably. Not only has his amazing ingenuity been a great relief in my times of need but his never-failing humor has lightened my mood numerous times. Michael was wonderful at helping me think more clearly and honestly about research problems. Kinu!!!!!!! :) She never failed to offer compassion and encouragement, two invaluable commodities at MIT. :) I have been so lucky to have Salil as an officemate; we have shared so much laughter and commiseration. This guy is going to go far, mark my words. And everyone else, Andy, Rooz, Stan, Jay, Betty and Abe, it's been a pleasure to work with everyone.

In the greater MIT community, I am grateful to Dr. Leeb, truly a prince, for teaching me how to fabricate the gels. Kurt Broderick, the wizard behind MTL, never failed to help me out with any problems I had. I am so grateful to Marilyn Pierce for always being so kind and confident in me.

I have to acknowledge a few friends that were simply essential to me. I would never have been at MIT if it weren't for John Wu. I am very grateful to him for encouraging me that I could make it at MIT and I better apply! And although he is far away in start-up land, dear Sri is virtually always reachable via cell for a mental and emotional caffeine boost. Dear Melissa is a true friend and even did her part with this thesis, helping me with grammar and organization. And Lin, Irina, Corina, Aarti and Kim, I am so glad for having these awesome girlfriends! Finally, there is no way I can acknowledge all the people who knowingly and unknowingly strengthened me on this journey. Thank you.

Last, I owe everything to my wonderful family. Thank you so much Mom and Dad for always loving me through the good and the bad times. And thank you to Alister, Olivia, Margaret and Stuart, my utterly adorable nephews and nieces for always being

so excited to see me. And thank you Matt, Michelle, Becky and Elizabeth for the love we have shared thus far and will share.

Contents

List of Figures

List of Tables

Chapter 1

Background and Motivation

Gels have been described as a "form of matter intermediate between a solid and liquid, (Tanaka, 1981)." Gels are mostly fluid with a matrix of polymer strands immersed in the fluid that gives the gel structure and form. The consistency of gels ranges from viscous fluids to somewhat rigid solids but typically they are soft and resilient, similar to the dessert Jello, which is perhaps the most familiar gel. Gel's have the notable characteristic of changing drastically in volume in response to infinitesimal changes in the surrounding environment.

Gels are of interest in a variety of fields. Gels are used as intermediates in manufacturing polymers such as rubber, plastics, glues and membranes. Many new applications are currently being investigated. Gels may also be useful for soft actuators and valves (Mitwalli, 1998). Gels are being modeled as artificial muscles (Woojin, 1996).

Many natural gels can be found in the human body as well. The vitreous humor that fills the interior of the eye, the material of the cornea, cartilage and the synovial fluid are all gels. Biological gels control the diffusion of oxygen, nutrients and other charged and uncharged molecules.

The tectorial membrane (TM) is a natural gel in the inner ear, overlying the sensory hair cells. The hair cells are the sensory receptors of the hearing process. The TM is in a strategic position to directly affect the sensitivity and frequency selectivity of hair cells.

There is compelling genetic evidence that the TM is needed for hearing. Mutations

of the genes TECTA and COL11A2 in mice are associated with an abnormal TM (Legan et al., 2000; McGuirt et al., 1999). Mutations of these same genes in humans are associated with hearing impairments (McGuirt et al., 1999; Verhoeven et al., 1998).

Although genetic research indicates the TM is crucial for hearing, there is little knowledge of how or why it is important. Many different models of the TM have been developed that are contradictory to each other. These models propose the TM is a rigid linkage (Davis, 1958), or a resonant mass (Zwislocki, 1979; Allen, 1980), or a completely isolated mass atop the hair bundles (Mammano and Nobili, 1993). These models are based on sparse experimental data (von Békésy, 1947; von Békésy, 1953; Zwislocki and Cefaratti, 1989; Abnet and Freeman, 2000). Since the TM is microscopic and 97% water, it has been difficult to perform experiments to characterize the TM.

By developing new experimental methods, our lab is measuring the TM's mechanical and electrical properties to develop a physically realistic model that relates the TM's function to the other hearing processes in the inner ear. Experiments to date fit well with a simple polyelectrolyte model for the gel (Freeman and Weiss, 1997). This model is characterized by two material constitutive relations - a stress-strain relation and a charge-concentration relation. These two relations are inherently interrelated.

The charge-concentration relation describes the interaction between fixed charges and mobile ions. The fixed charge concentration (C_f) is the quantity of ionizable non-mobile charge groups on the polymer network per unit volume of fluid in the gel. Mobile ions diffuse in and out of the gel. Because of the fixed charge, there is an electrical attraction for ions with the opposite charge and electrical repulsion for ions with the same charge. In addition, there are osmotic, mechanic and chemical forces acting on the mobile ions. Because of these forces, the concentration of each ion in a gel is different from that ion's concentration outside the gel, in the surrounding bath. This difference in ionic concentration causes a junction potential (EP) to develop between the gel and the surrounding bath as illustrated in figure 1-1.

By setting up an experiment with the gel in an ionic bath, measuring this EP and

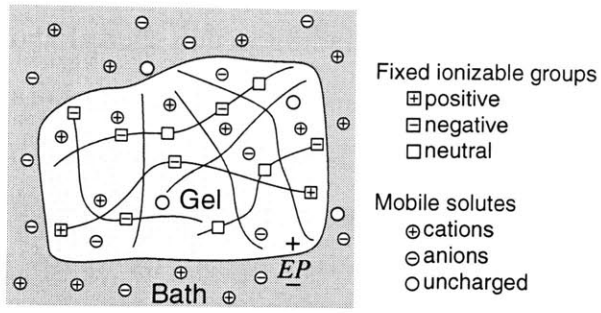

Figure 1-1: Polyelectrolyte gel and surrounding bath, adapted from (Freeman and Weiss, 1997). The gel's matrix has ionizable molecules (the squares) permanently attached to it. Mobile solutes (the circles) diffuse into the gel. Interactions between the mobile and fixed charged groups result in a junction potential, EP, at the gel-bath boundary.

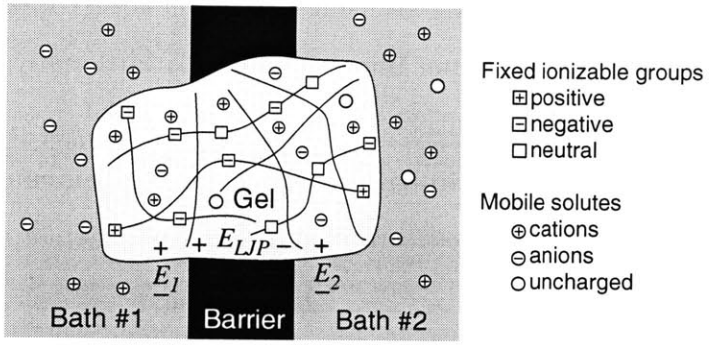

Figure 1-2: Two bath technique for measuring electrical properties of a gel as adapted from (McAllister, 1998). The gel contacts two baths separated by a barrier. Three potentials develop: E_1 at the gel interface with Bath 1, E_2 at the gel interface with Bath 2 and E_{LJP} through the gel.

using a model to relate C_f to EP, the C_f can be estimated. A number of technical difficulties complicate measurement of the EP between the gel and the bath. Because the TM is microscopic and is 97% water, it is very fragile and tears easily. It is difficult to insert an electrode into the center of the TM and not pierce completely through it and/or introduce tiny tears into the membrane.

To surmount these difficulties a two-bath method was developed in our lab (McAllister, 1998). The TM was positioned as the electrical connection between two baths (figure 1-2). The electrical potential between the baths is the difference between two gel-bath EPs plus a liquid junction potential. The gel-bath EPs are between the TM and bath 1 and between the TM and bath 2; the liquid junction potential is through the gel. Estimates of the C_f of the TM from this two-bath method using the Donnan Equilibrium Theory are roughly a factor of ten larger than any other C_f estimates (Freeman and Weiss, 1997).

The discrepancy between this estimate and previous estimates may be caused by

a number of factors. The C_f is dependent on a number of experimental conditions: pH of the surrounding bath, pressure on the gel, molecular binding within the gel and hydration of the gel. Alternatively, the discrepancy may be an artifact of the two-bath method. With the two-bath method, the majority of the TM is exposed to air between the two fluids. This is significantly different from its natural fluid environment. It is conceivable that the fluid in the TM evaporates during the experiment causing dehydration and shrinking. The reduction in volume will result in a larger C_f.

In this thesis, I investigated this theory of shrinking due to air exposure with an artificial polyelectrolytic gel. The principle advantage of using the artificial gel was that it could be custom fabricated with a known upper limit to its C_f. Additionally, the artificial gel can be fabricated reliably and repeatably.

The artificial gel's C_f was estimated using the two-bath method and the Donnan Equilibrium Theory. The size of the gel was measured throughout the experiment to correlate geometric changes with changes in C_f.

As a control experiment, the gel's C_f was estimated using the same two-bath method but with the gel insulated from the air by glass. This prevents the gel's C_f from changing due to exposure to air. The C_f estimates from the air-exposed two-bath experiment and the enclosed two-bath experiment were compared to the theoretical upper limit of the C_f.

Chapter 2

Theory and methods

This chapter describes the theory and methods used in this thesis. First, the Donnan Equilibrium Theory (DET) (Freeman and Weiss, 1997) used to estimate the artificial gel's C_f from its potential is described. Second, the two bath experimental technique is described. Because the artificial gel potential is small (less than 10 mV) and is measured in ionic solutions, special methods were used. These methods include using Ag/AgCl-salt gel electrodes and referencing the measured artificial gel potential to a potential measured with the two baths shorted by a salt gel bridge. Last, the fabrication steps of the artificial gel, the Ag/AgCl electrodes and the salt gel bridge are described.

2.1 Estimation of the fixed charge from a gel-bath voltage

The two-bath experimental setup for this thesis replicated the experimental setup in which the TM's C_f was estimated. The TM's normal environment is endolymph, a solution that predominantly contains K^+ and Cl^- ions. In the previous TM experiment, the ionic solutions in the baths were artificial endolymph (AE), K21, K43, K87 and K696. The solutions used to test this artificial gel were artificial endolymph (AE), K21, K43, K348 and K696. See table 2.1 for solution recipes. AE was an

approximation to endolymph. K21, K43, K348 and K696 were also endolymph approximations with varying KCL concentrations. Additionally, a NH_4Cl buffer, was added to all solutions to maintain a high (> 9.5) pH.

In this thesis the artificial gel's fixed charge concentration was estimated using the DET. The DET describes the relationship between 1) the concentrations of diffusable ions inside a gel, 2) the concentration of diffusable ions outside a gel in a surrounding ionic bath, 3) the fixed charge within the gel and 4) the junction potential created by all of these ions. Since the bath solutions are endolymph approximations, the only significant ions are assumed to be K^+ and Cl^- ions. The DET assumes a gel is in equilibrium and the concentrations of ions are unchanging inside and outside the gel. The DET consists of a set of fundamental relations which are described next.

Substance	AE	K21	K43	K87	K348	K696	K3000
KCl $\frac{mmol}{L}$	174	21	43	87	348	696	3000
NaCl $\frac{mmol}{L}$	2	2	2	2	2	2	2
CaCl $\frac{mmol}{L}$	0.02	0.02	0.02	0.02	0.02	0.02	0.02
NH_4Cl $\frac{mmol}{L}$	5	5	5	5	5	5	5
Dextrose $\frac{mmol}{L}$	3	3	3	3	3	3	3

Table 2.1: Compositions of solutions. Solutions are adjusted with KOH and HCl for 9.5≤pH≤10.5. Chemicals obtained from Aldrich Chemicals, Milwaukee, WI.

2.1.1 Electroneutrality in the gel

Electroneutrality states that the electrical charges in the bulk of a solution sum to zero. This principle holds both inside and outside the gel,

$$C_K^o - C_{Cl}^o = 0, \text{ outside the gel,} \tag{2.1}$$

and

$$C_K^i - C_{Cl}^i - C_f = 0, \text{ inside the gel.} \tag{2.2}$$

where C_f represents the fixed charge concentration of the gel, C_K^i and C_{Cl}^i represent the concentration of potassium and chlorine in the gel, respectively and C_K^o and C_{Cl}^o

represent the concentration of potassium and chlorine in the bath, respectively. C_f is subtracted in equation 2.2 because although, C_f is positive, the fixed charge is known to be negative.

2.1.2 Electrodiffusive equilibrium

When measured in a single bath, electrodiffusive equilibrium exists across the gel-bath interface. The fixed charge in the artificial gel exerts an electro-motive force on the mobile ions in the bath solution, attracting ions of opposite charge and repelling ions of similar charge. This flux is opposed by a diffusive flux down the concentration gradients. This equilibrium condition relates the concentration of K^+ ions and C^- ions inside and outside the gel. These ionic concentrations have a specific ratio and cause a junction potential which is expressed as

$$V = \frac{kT}{q} \ln \frac{C_K^o}{C_K^i} = \frac{kT}{q} \ln \frac{C_{Cl}^i}{C_{Cl}^o}, \tag{2.3}$$

where k is Boltzmann's constant, T is the absolute temperature, and q is the charge of one proton. The relationship can be manipulated and generalized for the nth ionic species as,

$$C_n^i = C_n^o (e^{\frac{-Vq}{kT}})^{z_n} = C_n^o d^{z_n}, \tag{2.4}$$

where z_n is the valence of the nth ionic species and $d^{z_n} = e^{\frac{-Vqz_n}{kT}}$. Since the only ions being accounted for are K^+ and Cl^-, $z_n = \pm 1$.

Equation 2.2 and equation 2.4 are combined to give the quadratic function

$$d^2 + d\frac{C_f}{C_K^o} - \frac{C_{Cl}^o}{C_K^o} = 0. \tag{2.5}$$

Solving equation 2.5 yields,

$$d = -\frac{C_f}{2C_K^o} \pm \sqrt{(\frac{C_f}{2C_K^o}^2 + \frac{C_{Cl}^o}{C_K^o})}. \tag{2.6}$$

The positive solution is used because d, the ratio of two positive numbers, must

be positive. The voltage at the gel-bath interface is now expressed as a function of C_f, C^o_{Cl} and C^o_K,

$$EP = \frac{kT}{q} \times \ln\left(\sqrt{\left(\frac{C_f}{2C_{bath}}\right)^2 + 1} - \frac{C_f}{2C_{bath}}\right). \tag{2.7}$$

where $C_{bath} = C^o_K = C^o_{Cl}$.

Equation 2.7 shows that a gel's C_f could be estimated by measuring the gel-bath EP. However, in the case of the TM, it is very difficult to reliably measure this EP with microelectrodes. To overcome this problem, the two-bath technique was developed.

2.2 Estimation of the fixed charge when using the two-bath technique

In the two-bath method, a gel is used as the electrical connection between two baths (figure 1-2). Two gel-bath EPs develop; one EP between the gel and bath 1 and another EP between the gel and bath 2. By assuming the DET, the measured potential, V_d, is assumed to be the difference between the two gel-bath EPs and is given by,

$$V_d = \frac{kT}{q} \times \ln\left(\frac{\sqrt{\left(\frac{C_f}{2C_{bath_1}}\right)^2 + 1} - \frac{C_f}{2C_{bath_1}}}{\sqrt{\left(\frac{C_f}{2C_{bath_2}}\right)^2 + 1} - \frac{C_f}{2C_{bath_2}}}\right). \tag{2.8}$$

C_{bath_1} was a reference bath and contained artificial endolymph (AE). C_{bath_2} was the test bath. It was alternately K21, K43, K348 and K696. There are two methods for determining C_f. The first method estimates C_f directly from equation 2.8 by substituting the measured V_d, C_{bath_1} and C_{bath_2}. In the second method, the potential difference for each test bath concentration was measured. The value of C_f that minimized the difference between the measured potentials and equation 2.8 in a least squares sense was chosen.

2.3 Effect of liquid junction potentials

The voltage measured by the voltmeter is the sum of V_d and all other solid and liquid junction potentials. Solid and liquid junction potentials occur anywhere there is a junction of dissimilar materials. A better assumption of the measured voltage is not only V_d as given in equation 2.8. Instead, the measured potential, V_l is expressed as,

$$V_l = V_1 + V_2 + V_d - V_3 - V_4, \tag{2.9}$$

where V_1 and V_4 are the solid junction potentials between the Ag/AgCl electrodes and surrounding salt gel. V_2 is the liquid junction potential between the salt gel and test bath. V_3 is the liquid junction potential between the salt gel and reference bath (AE). V_d is as defined in equation 2.8. Figure 2-1 illustrates the loop measured by the voltmeter.

V_1 and V_4 have been found empirically to be (Ives and Janz, 1961)

$$V_1 = V_4 = V_o^{Ag/AgCl} - \frac{kT}{q} \ln C_{Cl} \tag{2.10}$$

where C_{Cl} is the concentration of Cl^- ions in the salt gel. $V_o^{Ag/AgCl}$ is the "standard electrode potential," and is a function of the electrode. It should theoretically subtract out when using two Ag/AgCl electrodes of identical composition. This equation shows that the potential created is theoretically non-polarizable and reversible. Non-polarizable means the potential is unaffected by the current flow. Reversible means that the v-i characteristic is ohmic with no hysteresis. Both Ag/AgCl electrodes are made with the same salt gel, K3000 (see table 2.1). Thus, the same concentration of chlorine is used in equation 2.10 for estimating V_1 and V_4 and the two potentials theoretically cancel each other.

The potential for V_2 is defined as (Weiss, 1996),

$$V_2 = \frac{kT}{q} \left(\frac{\mu_K - \mu_{Cl}}{\mu_K + \mu_{Cl}}\right) \ln \frac{C_{testbath}}{C_{saltgel}}, \tag{2.11}$$

where μ_K is the mobility of K^+ ions and μ_{Cl} is the mobility of Cl^- ions. Likewise,

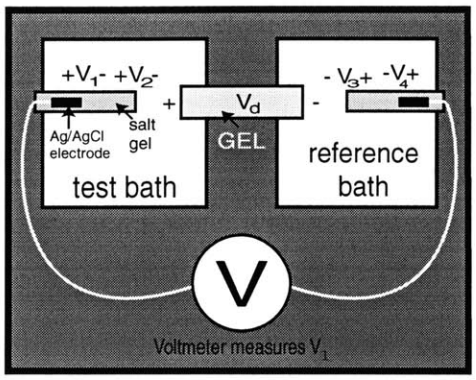

Figure 2-1: Schematic diagram illustrating additional junction potentials occurring in measurement of gel voltage. The voltmeter is represented by a "V." The large white squares represent the test bath and reference bath dishes. The gray rectangle in the center represents the gel; it produces a voltage, theoretically modeled as V_d from equation 2.8. The smaller black rectangles within larger gray rectangles represent Ag/AgCl electrodes and the surrounding salt gel, respectively. The white lines represent the connection between the voltmeter and the electrodes. The additional junction potentials, V_1, V_2, V_3 and V_4 are indicated.

the potential for V_3 is defined as,

$$V_3 = \frac{kT}{q}\left(\frac{\mu_K - \mu_{Cl}}{\mu_K + \mu_{Cl}}\right) \ln \frac{C_{referencebath}}{C_{saltgel}}. \tag{2.12}$$

V_2 and V_3 do not cancel each other since $C_{testbath} \neq C_{referencebath}$. The values for $V_2 - V_3$ for the four solutions are shown in table 2.3. Thus, in the results, the measured gel voltages are assumed to be,

$$V_l = V_d + V_2 - V_3, \tag{2.13}$$

where V_d is defined in equation 2.8.

Solutions	$V_2 - V_3$ [mV]
K21-AE	1.02
K43-AE	0.68
K348-AE	-0.33
K696-AE	-0.67

Table 2.2: Liquid junction potentials between test bath solutions and reference bath (AE).

2.4 Shorting method to reduce uncontrolled voltage variations in two-bath technique

A number of uncontrolled factors (such as temperature) can also affect the voltage measured in the two-bath method. We represent the effect of these factors as a voltage $V_{extra}(t)$ that is added to V_l (equation 2.13) as follows,

$$V_{l2}(t) = V_l + V_{extra}(t). \tag{2.14}$$

To estimate $V_{extra}(t)$, the baths are shorted together with a salt gel shorting bridge with the same KCl concentration (K3000) used in the salt gel electrodes. When the baths are shorted, all junction potentials defined in section 2.3 theoretically cancel each other thus the resulting voltage is, $V_s(t) = V_{extra}(t)$. Ideally, $V_{l2}(t)$ and $V_s(t)$ would be measured at the same time so the extraneous voltages could be subtracted out perfectly. The following voltage difference was the experimental voltage compared with the theoretical voltage defined in equation 2.13.

$$V_g(t) = V_{l2}(t) - V_s(t + \delta), \tag{2.15}$$

where δ was the time between measuring the gel and the short.

2.5 Measurement method for the enclosed and air-exposed two-bath technique

2.5.1 Apparatus

The 4 major components of the experimental setup were the two-bath chamber, the perfusion system, the voltage acquisition system, and the gel. The two-bath chamber (figure 2-2) consists of two plastic tissue culture dishes (Becton Dickinson, Franklin Lake, NJ) each with a diameter of 35 mm and a depth of 10 mm. They are placed a distance of 1.15 mm from each other. The gel bridged this gap. One dish contained

Figure 2-2: The chamber consisted of two dishes placed a distance of 1.15 mm from each other. The left dish contained AE, the reference fluid. The right dish contained one of the test solutions, K21, K43, K348 or K696. The gel straddled the two dishes such that each end of the gel dangled in one of the two baths.

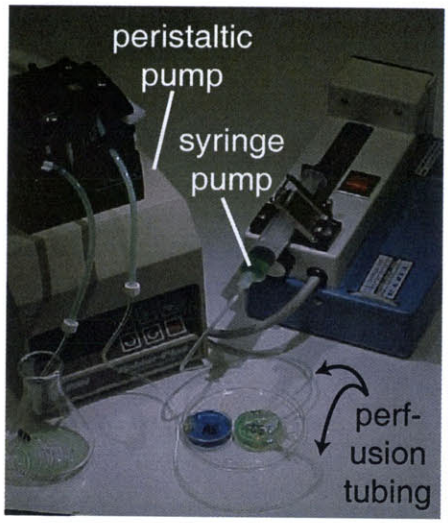

Figure 2-3: The chamber with the perfusion system connected to the test bath. A peristaltic pump, shown on the left, was used for the outflow. The inflow was controlled by a motorized syringe pump (right).

the reference solution, AE. The other dish contained one of the test solutions: K21, K43, K348 or K696.

The test bath was perfused to eliminate an ionic stagnation layer at the gel-bath interface. Syringes mounted on a pumping system (Razel, Stanford, CT) were used for inflow and peristaltic pumps (Rainin Instrument Co., Woburn, MA) were used for outflow. A large chunk of polydimethylsiloxane, PDMS, (Sylguard 184, Dow Corning, Midland, MI) was fixed in the test bath to force the solution to flow very close by the gel and not through the center of the dish. The reference bath was not perfused. The two-bath chamber with the perfusion system is shown in figure 2-3.

The voltage acquistion system consisted of a Tektronix TX3 voltmeter (Beaverton, OR), amplifier (DAM 60, World Precision Instruments, Sarasota, FL) and Ag/AgCl electrodes in a highly conductive (K3000) salt gel solution. A computer acquired and saved the voltages from the amplifier. The amplifier was needed because the

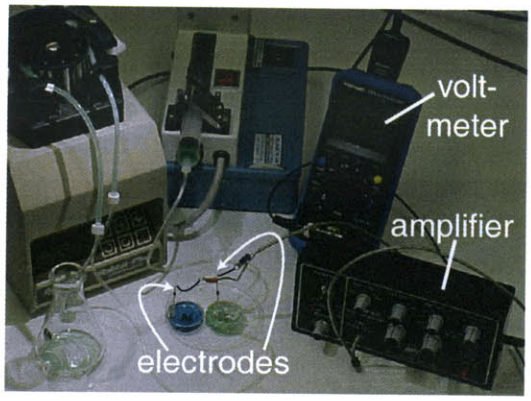

Figure 2-4: The voltage acquisition system is shown with the perfused two-bath chamber. Ag/AgCl electrodes in salt gel contacted each bath. The voltage across the two baths was amplified, then read by the voltmeter and sent via the serial port to an IBM compatible computer.

gel-bath potential ranged from 1 mV to 8.5 mV and was close to the noise floor of the voltmeter. The two-bath system with the perfusion system and the voltage acquisition system is shown in figure 2-4.

The gel was a solid cylinder with a diameter of about 340 μm. The gel was balanced on the edge of the two dishes contacting AE on one side and the test solution on the other side. Thus, the gel provided the only electrical connection from the reference bath to the test bath.

There were two sets of experiments performed, one in which the gel was enclosed and one in which the gel was exposed to air. For the enclosed measurements, none of the gel was exposed to air. A middle section of the gel was entirely enclosed by a glass cylinder. The gel protruded on each side from this middle glass section. The glass cylinder rested so one end of it was on the edge of the test bath and the other glass end rested on the edge of the reference bath. The gel that protruded from the glass dangled in one of the baths. The enclosed gel with the two-bath chamber is shown in figure 2-5.

For the air-exposed measurements, the gel straddled the test bath and the reference bath similar to the enclosed measurements. Although the majority of the gel was in solution the middle section was not enclosed within a glass cylinder. This left approximately 1.15 mm exposed to air.

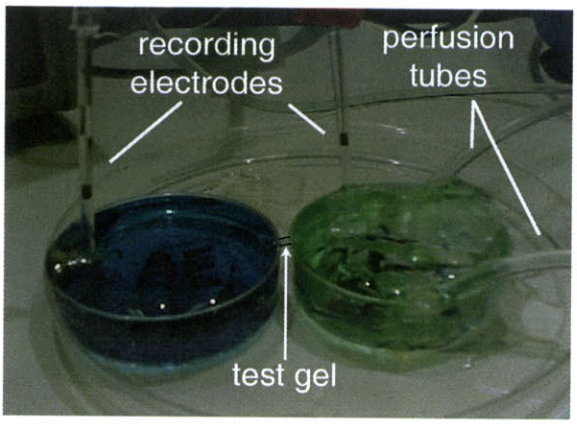

Figure 2-5: The glass-enclosed gel straddled the test bath and the reference bath. A Ag/AgCl/salt gel electrode was in each bath to measure the potential. Inflow and outflow perfusion tubes were in the test bath. A large chunk of PDMS was inserted into the test bath to force the fluid to flow past the gel.

2.5.2 Two-bath Protocol

The first step was to prepare the baths. The reference bath dish was filled with AE until there was a convex meniscus of AE above the dish edges. The test bath was filled the same way with one of the 4 test solutions.

The next step was to get steady inflow and outflow of the test solution with the perfusion system. The inflow and outflow tubes are threaded through epoxied rubber rings on the dishes so that the tubes stay fixed during an experiment. Typical perfusion rates were 27 mL/hour for both inflow and outflow.

Following this, the voltage acquisition system was added to the setup. The voltmeter was hooked up to the serial port of the computer. The voltmeter and the amplifier were also connected together. The amplifier's gain was set to ten and the DC offset was adjusted to zero. The silver wires extending from the electrodes were each wrapped around the amplifier leads. The glass-enclosed electrodes were inserted into epoxied rubber rings on the dishes to keep them fixed during the experiment. The voltage acquisiton computer program was started.

Last the gel was placed between the two dishes. In the case of the enclosed gel, the gel was placed carefully on the dish edges such that the gel extending out of the glass was not exposed to air. Following placement of the gel, the gel's potential would be monitored. For acquistion of the shorted potential, the shorting bridge would be

placed in parallel with the gel.

2.5.3 Three-bath Protocol

A three-bath method was initially used to measure artificial gels with a 1.0 mm diameter. Because this diameter is equal to that of the shorting bridge, when the shorting bridge was placed in parallel with the gel, the voltmeter did not record a short. Empirically determined, for the shorting bridge to short out the gel when placed in parallel, the shorting bridge needed to have a cross-sectional area at least 12.5 times larger than the gel's cross-sectional area.

The protocol for the three-bath method is the same as the protocol for the two-bath method except three baths are used. In the three-bath method, the test solution filled two of the baths. The third bath had the reference solution. The electrodes were in test bath 1 and the reference bath. The gel was across test bath 2 and the reference bath. Test bath 2 was perfused. For the gel potential measurement, the shorting bridge was placed across test bath 1 and test bath 2. For the shorted potential, the shorting bridge was placed across test bath 1 and the reference bath. Because of this method, during the switching of the shorting bridge, the voltmeter recorded an open circuit potential.

2.6 Estimation of geometric changes in the gel

In the air-exposed two-bath technique, gel images and gel voltages were acquired simultaneously. Section 2.6.1 describes the equipment and methods used to acquire the images. Section 2.6.2 describes how images of the gel were used to estimate changes in the volume of the gel.

2.6.1 Measurement methods for image acquisition

The gel was imaged with a 6.3x objective (Zeiss, Oberkochen, Germany) on a compound microscope (Zeiss WL, Oberkochen, Germany). Brightfield images were ob-

tained with transillumination. A piezoelectric focusing device (PIFoc P-721, Physik Instrumente, Waldbronn, Germany) brought different planes of the gel into focus. The PIFoc moved a depth of 100 μm and images were collected every μm with a scientific grade CCD camera (TM1010, PULNiX, Sunnyvale, CA). The time-stamped 1000×1016 pixel images were stored on an IBM-PC compatible computer running custom software for the Linux operating system.

During an experiment, each time the image acquisition program was run, 100 images of the gel at different focal planes were acquired. Of these images, there was a subset of the images where the gel was the most clearly in focus. Of this subset, the one that appeared the most clear was selected for measurements.

2.6.2 Estimation of volume changes

The method used to estimate changes in the gel's volume was based on the shape to which it typically shrunk. The shrunken volume was estimated as being two partial cylindrical cones with a small cylinder between the two cones, as shown in figure 2-6. For this calculation, 4 dimensions were measured: r_0, the outer radius, r_1, the inner radius, L_1, the length of the conic sections and L_2, the length of the cylinder. The distances were measured in pixels using a custom software program. The pixel units were converted to μm based on the magnification. The equation for the gel volume was

$$V_n = \frac{2}{3}\pi(r_0^2 + r_1^2 + r_0 r_1)L_1 + \pi r_1^2 L_2. \tag{2.16}$$

The non-shrunken volume was

$$V_o = \pi r_0^2(2L_1 + L_2). \tag{2.17}$$

The shrunken volume was normalized by the non-shrunken volume,

$$\beta = \frac{V_n}{V_o}. \tag{2.18}$$

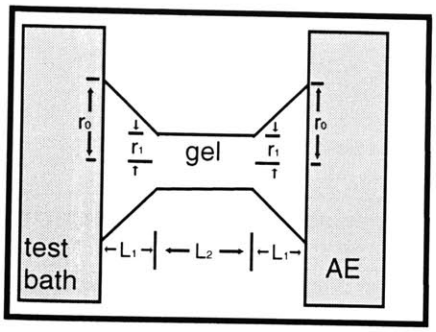

Figure 2-6: Approximation of shrunken gel volume during two-bath experiment. The gray boxes represent the reference and test bath dish edges. The shrunken gel is represented in the middle. The 4 dimensions that are measured are indicated.

2.7 Comparison between air-exposed gel's C_f and normalized volume

In comparing the air-exposed gel's C_f with the normalized volume, the data from each test bath were analyzed individually. Thus, instead of doing a least squares fit, equation 2.15 was manipulated to find the estimated C_f from a measured potential difference.

Initially, $C_{f_o} = \frac{N_f}{V_o}$, where C_{f_o} was the unexposed fixed charge concentration, N_f was the number of fixed charges in the gel and V_o was the unshrunken volume defined in 2.6.2. For the gels used in this thesis, it was assumed that N_f remained constant. After the gel was exposed, $C_{f_n} = \frac{N_f}{V_n}$, where C_{f_n} was the air-exposed estimated fixed charge concentration and V_n was the shrunken volume defined in 2.6.2. These two relations were combined as

$$C_{f_n} = \frac{1}{\beta} C_{f_o} \tag{2.19}$$

where β was as defined in equation 2.18.

The estimates of C_{f_n} and $\frac{1}{\beta}$ were plotted and a straight line was fit to the data. The slope of this line was defined as $C_{f_o}^{experimental}$. The data were compared to another line that had a slope equal to the enclosed gel's median estimated C_f and an intercept equal to zero. The slope of this line was defined as $C_{f_o}^{enclosed}$.

2.8 Fabrication of the gel

2.8.1 Chemistry

The gel used in this thesis is a mesh of long-chain polyacrylamide formed from two monomers (acrylamide and bisacrylamide), sodium acrylate, ammonium persulfate (APS) and tetramethyl ethylene diamine (TEMED) (Tanaka, 1981). Acrylamide is a small organic molecule that terminates in an aminocarbonyl ($-CONH_2$) group. Bisacrylamide consists of two acrylamide monomers linked through their aminocarbonyl group. Each molecule of sodium acrylate has a dangling carboxyl ($-COOH$) group. This carboxyl group can ionize and form $-COO^-$, giving the gel a fixed charge. Acrylamide, bisacrylamide and sodium acrylate are dissolved in AE. The addition of APS and TEMED to the solution causes a chain reaction which forms the long-chain molecules.

The gel formation process begins with a reaction between APS and TEMED leaves the TEMED molecule with an unpaired electron. The activated TEMED molecule combines with an acrylamide or bisacrylamide monomer. Because of this, the unpaired electron is transferred to the acrylamide unit making it reactive. Another monomer or a sodium acrylate molecule can then be attached and activated in the same way. By shifting the active site to the end of the chain, the polymer continues to grow indefinitely until the supply of monomers and sodium acrylate is exhausted.

Acrylamide and bisacrylamide combine to produce a cross-linked matrix of long-chains. Acrylamide monomers can only combine to one active site at a time and hence they can only form long, unbranched chains. But bisacrylamide can combine to two chains at once, creating cross-links.

Bisacrylamide is also needed to give stiffness to the gel. Stiffness helps decrease swelling of the gel. A number of methods were optimized to prevent the gel from changing size due to factors not related to air exposure. As the amount of bisacrylamide is increased, the polymers are more tightly bound together and more strongly resist any force that pulls them apart.

The concentration of sodium acrylate in the gel is 31.5 $\frac{mmol}{L}$. A certain percentage

of the sodium acrylate will ionize depending on the pH of the gel. If all the sodium acrylate ionized, the fixed charge concentration would be -31.5 $\frac{mmol}{L}$.

C_f was chosen to be less than 31.5 $\frac{mmol}{L}$ for two reasons. First and most important, this value is close to previously estimated values for the TM, which are in the range 6.4 $\frac{mmol}{L}$ to 18 $\frac{mmol}{L}$ (Freeman and Weiss, 1997). Second, to decrease osmotic swelling, C_f should be as small as possible. Because of the gel's C_f, the concentration of the mobile ions will always be greater within the gel than the surrounding bath. As C_f increases, the mobile ion concentration difference increases from inside to outside the gel; this results in the gel swelling more.

The chemistry of the gel was further defined with AE of pH > 9 as the solvent. During the two-bath experiment, one of the two baths was always AE with a pH > 9. When a gel made with DI water is placed between AE and another high pH ionic solution, the equilibration of the gel with the baths causes a change in the gel size. To prevent this, the gel was made with AE.

2.8.2 Fabrication steps

The fabrication steps were adapted for this thesis (Mitwalli, 1998). The first step was to start with the correct protective equipment. No chemical in this preparation was without its warning. "Cancer suspect agent! Toxic! Irritant! Neurologic hazard! Mutagen! Possible Teratogen! Readily absorbed through skin! Avoid contact and inhalation!" This was the warning on the label for just one of the chemicals, acrylamide. Non-disposable rubber gloves, lab coat, goggles and a functioning hood were necessary safety precautions.

The second step was to start with clean equipment. The consistency and repeatability of the gels was very sensitive to the fabricating conditions. All glassware were washed with Pex, rinsed with DI water, and let dry.

The last step before mixing the chemicals was to prepare the container in which the gel will solidify. The gel solution could have been poured into any container and it would solidify in that form. For this thesis, the gel solution was poured into 16 × 100 mm test tubes. Before pouring the gel solution into the test tube, 5 μL glass pipets

(Drummond Scientific, Broomall, PA) were inserted into the test tube. When the gel solution was poured into the test tube, capillary action drew the solution up the 5 μL pipets. From these glass pipets, the pieces of gel used in the test were obtained.

There were two mixtures prepared. In the first mixture, 0.2 g APS (Aldrich Chemicals, Milwaukee, WI) was dissolved in 5 mL AE. The solution was mixed well and then deoxygenized using either of the following two methods. One method was to place the entire solution in an enclosed space and apply a vacuum to the enclosed space. Another method was to blow a small stream of nitrogen gas (less than 40 psi) into the base of the solution's container for at least a minute. This saturated the solution with nitrogen. Because nitrogen is heavier than oxygen, it pushed all the oxygen out of the solution. Following this, the solution was covered with parafilm and set aside.

In the second mixture, 0.75 g acrylamide, 0.03 g sodium acrylate, and 0.078 g bisacrylamide (Aldrich Chemicals, Milwaukee, WI) were dissolved in 9.9mL AE. The solution is mixed well and deoxygenized after adding 0.1 mL plain (uncharged) fluorescent beads (Polysciences, Inc., Warrington, PA) to it.

To initiate the reaction, 24 μL TEMED and 100 μL of the first APS solution were added to the second solution. The solution was then gently mixed for ten seconds. The solution was poured into the prepared test tube, parafilm was wrapped around top of test tube and the tube was set in a dark location for 20 hours.

If the steps were followed correctly, the gel solidified after 20 hours. The solid gel was no longer chemically hazardous. If it had not solidified, it was hazardous waste and needed to be treated accordingly. In case the reaction did not reach full completion, the gel was rinsed well with AE and handled carefully.

To remove the gel from the test tube, water was forced into the bottom of the test tube and the entire gel was pushed out. To begin, a long sharp metal object was carefully inserted to the bottom of the test tube. It was inserted near the perimeter of the tube. The metal object was moved around to slightly dislodge the gel from the test tube and removed. A 60 mL syringe was filled with AE or DI water and a long disposable glass pipette was attached to it. The tip of the pipette was inserted

into the gel where the metal object had been. Fluid was carefully pumped into the test tube. If the resistance to pumping was too large, the glass pipette was removed, and the metal object was reinserted to loosen the gel a little more. This process was repeated until the gel began to loosen from the tube and could be pushed out of the test tube. The gel was then rinsed well with AE.

After rinsing, the gel was covered and stored in the refrigerator. The gel could not be placed in any solution because then it would tend to slide out of the small glass capillary tubes. With these fabrication steps, the gel was consistent in its electrical and handling properties for at least a month.

2.9 Fabrication of the shorting salt-gel bridge

2.9.1 Chemistry

The salt gel was a highly concentrated solution of KCl mixed with agarose. Upon heating the solution, it thickened and formed a substance with the consistency of soft margarine. The salt gel could not bridge and short the two dishes without falling apart. It was fabricated inside curved glass capillary tubes to bridge the two dishes.

2.9.2 Fabrication Steps

The first step was to prepare the glass capillary tubes. Glass capillary tubes with a 1.15 mm inner diameter and roughly 15 mm long were used (GC200-15, Warner Instrument Co., Hamden, CT). The tubes were curved by bending them while holding them over a bunsen flame. Each glass tube was held with two rubber handled pliers spaced roughly 5 mm apart on the tube. The tube between the two pliers was placed in the flame. When the glass started glowing, it was bent into a half moon shape. This process was repeated for the next 5 mm of the glass tube and then again for the last 5 mm of the glass tube. After the glass tube cooled down, it was broken into 3 pieces for 3 bridges. This process was repeated until 6 to 9 bridges were fabricated.

The next step was to heat the solution of 1.5 g agarose (Aldrich Chemicals, Mil-

waukee, WI) dissolved into 50 mL K3000. See table 2.1 for K3000 solution recipe. The solution was heated on a hot plate with a magnetic stirrer. To test if the solution was heated enough, small quantities of the solution were poured on a glass plate every 5 minutes or so (more often when the solution began steaming). When ready, the solution would gel quickly on the glass plate.

Once the solution was ready, it was important to work quickly before the solution had gelled in the container in which it was heated. A 60 mL syringe (Becton-Dickinson, Franklin Lakes, NJ) had a piece of rubber tubing (96429-34 Tygon, Cole-Parmer, Vernon Hills, IL) fit to its tip. The other end of the tubing was alternately fit to each glass piece. When the glass piece was inserted into the hot agarose-KCl solution, the syringe was used to suck the hot solution up into the glass. The syringe and rubber tubing were then carefully removed from this bridge and the process was repeated for all bridges. The solution solidified inside the glass bridges upon cooling. After sucking up the solution into all the tubes, the tubes should be wiped off and stored in K3000 in the refrigerator. When correctly fabricated and refrigerated, the bridges would last 3-4 weeks before dissolving.

2.10 Fabrication of the Ag/AgCl salt gel Electrode

The fabrication of the Ag/AgCl salt gel electrodes was similar to the fabrication of the shorting salt gel bridges. The first step was to prepare the glass capillary tubes with the Ag/AgCl electrodes. Glass capillary tubes with a 1.15 mm inner diameter and roughly 15 mm long were used. The tubes were broken into 3 pieces, each roughly 5 mm long. Ag/AgCl electrodes with a diameter of 1.0 mm (550010, A-M Systems, Carlsborg, WA) were inserted halfway down the tubes so that the electrode lead was sticking out of one glass tube end. This lead was folded over the glass tube end. A piece of tubing (96429-34 Tygon, Cole-Parmer, Vernon Hills, IL) was fitted over this folded lead and the glass tube end.

The same agarose-KCl solution used for the shorting bridges was used for the electrodes. Similar to making the shorting salt gel bridges, a 60 mL syringe was used

to suck the hot agarose-KCl solution up into the prepared glass tubes. The only difference from the shorting bridges was that each tube for the electrodes had its own piece of tubing whereas when making the shorting bridges, one piece of tubing could be reused.

Chapter 3

Measurements of enclosed and air-exposed gels

3.1 Enclosed measurements

3.1.1 Shorted two-bath voltages

Figure 3-1 shows voltages acquired when two baths, K696 and AE were shorted together. This voltage was not zero and was not constant. For over an hour, it was increasing at a steady rate of 5 mV/hour. As described in section 2.4, this voltage is due to potentials other than the gel's potential. This voltage was different from one experiment to the next. These potentials were caused by numerous things, convection in the fluid, temperature variations, diffusion of contamination ions, etc. In the case of this experiment, if the gel was measured without referencing it to this shorted value then it would appear that the gel's voltage was increasing at a rate of 5 mV/hour in addition to the actual gel voltage. Figure 3-2 shows the shorted voltage plus the gel voltage below it. By looking at the difference between the gel potential and the shorted potential in this experiment and in all experiments, the voltage is much more reliable, repeatable and accurate.

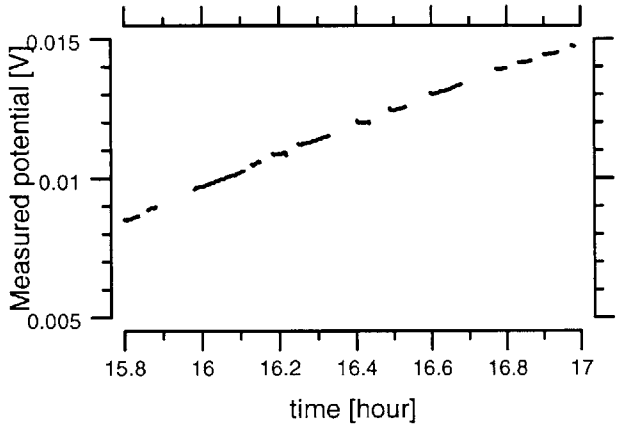

Figure 3-1: Measurement of potential as a function of time. The potential is due to shorting a test bath of K696 and a reference bath of AE with a 3 M KCl salt gel shorting bridge. Because the potential wasn't measured continuously, there are breaks in the measurements.

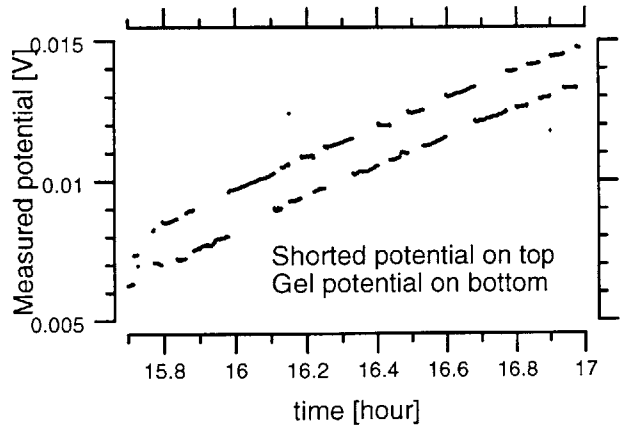

Figure 3-2: Measurement of potential as a function of time. The two-bath potential of the artificial gel was measured alternately with the potential of the two-baths shorted. The potential measurements consisting of the top sequence are the shorted two-bath potentials and also the same measurements as in figure 3-1. The potential measurements that consist of the bottom sequence are the gel's potential.

3.1.2 Potential measurements before perfusion

Figure 3-3 shows data taken with the three-bath technique before perfusion was incorporated into the technique. At 14.15 hours, the test solution was changed from K21 to K43. When the test solution was K21, the voltage difference increased to about 5.5 mV and then began decreasing. For a test bath of K43, the voltage averaged a little less than 3 mV. The test bath of K21 elicited a larger potential than the potential elicited with the test bath of K43. This is consistent with the qualitative notion that the increase in KCl concentration shields the fixed charges in the gel to reduce the potential. The gel's potential also had a positive polarity which is consistent with the gel having a negative fixed charge.

The potential measured for the gel exhibited a transient immediately after switching to it and removing the short. This transient was attributed to a stagnation layer that developed at the junction between the gel and bath when the switching and movement of the solutions ceased. A stagnation layer decreases the sharp concentration difference from gel to bath, and hence decreases the junction potential, as theorized in equation 2.3. When the test bath was perfused the voltage difference increased as seen in the next subsection.

3.1.3 Potential measurements after perfusion

Figure 3-4 shows the voltages acquired for a two-bath experiment with a perfused test bath. Similar to figure 3-3, the gel's potential difference was measured for K21 and K43. A comparison of perfused and non-perfused potential differences for both K21 and K43 is shown in figure 3-5. For both test bath solutions, K21 and K43, a larger potential difference was measured when the test bath was perfused and the perfused potential differences vary less.

A second perfused experiment for K21 and K43 is shown in figure 3-6. Although there is more voltage drift, the voltage differences are relatively constant and similar to the differences in figure 3-4. The differences remained relatively constant for each test bath for more than 2 hours.

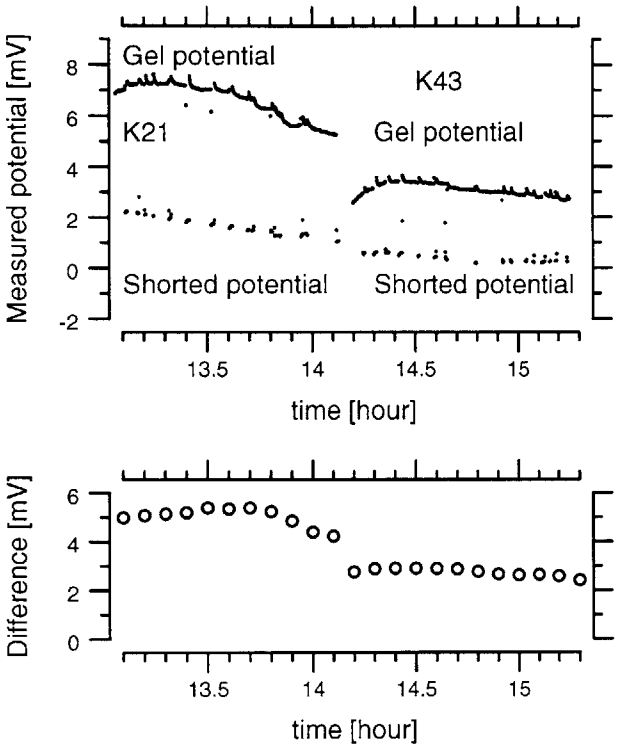

Figure 3-3: Measurements of the three-bath potential as a function of time for different concentrations of KCl in the test bath. The reference bath contained AE. At 14.15 hours, the test bath was switched from K21 to K43. The larger potential, measured when the gel was across the two baths is labeled 'gel potential.' The smaller potential, close to zero and labeled 'shorted potential,' was measured when the two baths were shorted. The lower graph shows the corresponding calculated differences between these measured shorted and gel potentials.

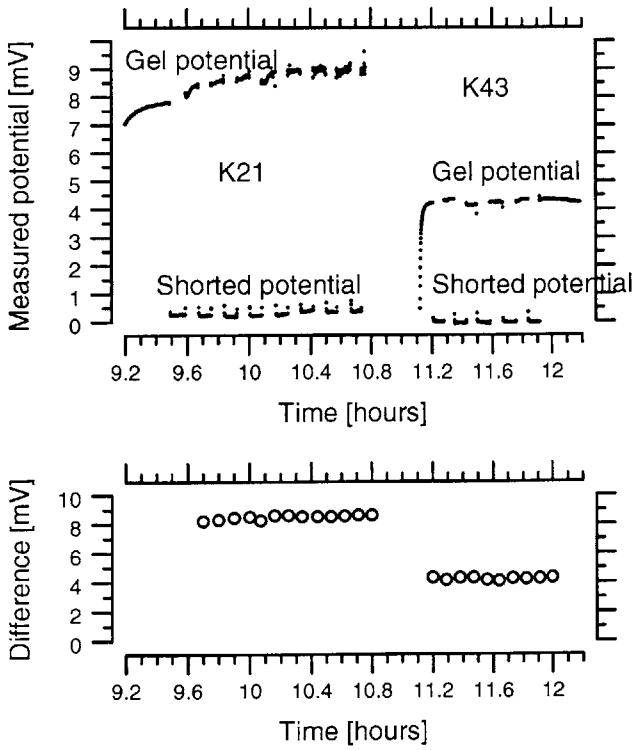

Figure 3-4: Measurements of the two-bath potential as a function of time for different concentrations of KCl in the test bath. The reference bath contained AE. At 11.0 hours, the test bath was switched from K21 to K43. The larger potential, measured when the gel was across the two baths is labeled 'gel potential.' The smaller potential, close to zero and labeled 'shorted potential,' was measured when the two baths were shorted. The lower graph shows the corresponding calculated differences between these measured shorted and gel potentials.

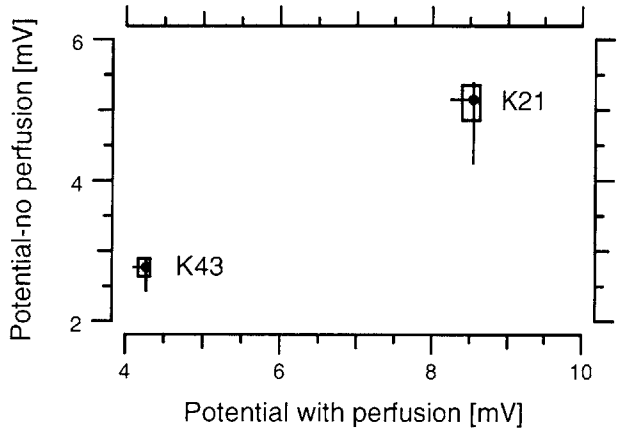

Figure 3-5: Comparison of measured potential differences for a perfused and a non-perfused test bath. The data for the perfused and the non-perfused are represented as box and whisker plots. The box indicates the interquartile range, the circles represent the medians and the vertical and horizontal lines span the entire non-perfused and perfused data, respectively. The test bath solution for each comparison is indicated next to the box.

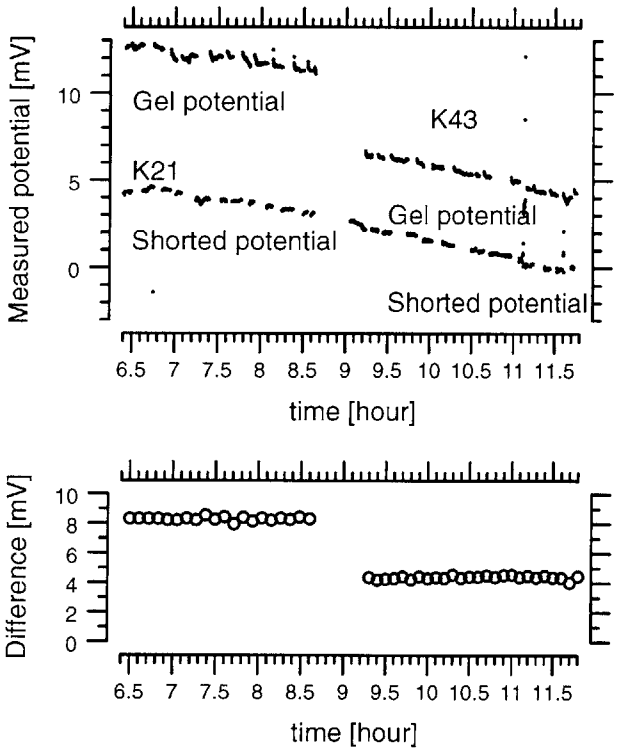

Figure 3-6: Measurements of the three-bath potential as a function of time for different concentrations of KCl in the test bath. The reference bath contained AE. At 8.8 hours, the test bath was switched from K21 to K43. The larger potential, measured when the gel was across the two baths is labeled 'gel potential.' The smaller potential, close to zero and labeled 'shorted potential,' was measured when the two baths were shorted. The lower graph shows the corresponding calculated differences between these measured shorted and gel potentials.

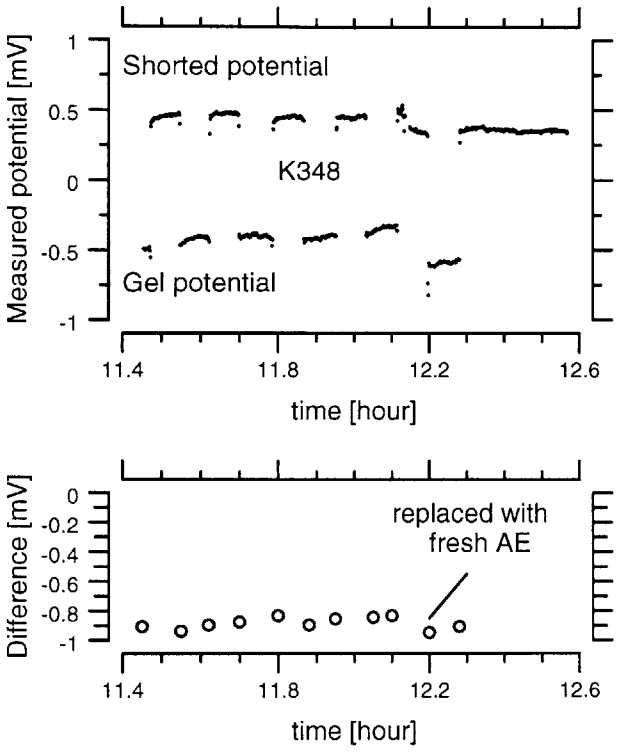

Figure 3-7: Measurements of the two-bath potential as a function of time with the test and reference bath as K348 and AE, respectively. The negative potential, measured when the gel was across the two baths is labeled 'gel potential.' The positive potential, close to zero and labeled 'shorted potential,' was measured when the two baths were shorted. The lower graph shows the corresponding calculated differences between these measured shorted and gel potentials.

Figure 3-7 and figure 3-8 show results from two-bath and three-bath experiments respectively. K348 was the test bath. The referenced gel potential, the difference, is negative. This switch from a positive potential to a negative potential was consistent with the test bath switching from having a smaller KCl concentration than the reference bath to having a greater KCl concentration than the reference bath. In figure 3-7 the drop in voltage at 12.2 hours was due to getting new AE for the reference bath. Figure 3-8 shows the voltage difference decreasing over the course of the experiment.

Figure 3-9 shows data taken during a three-bath experiment when K696 was the test bath. As seen in figure 3-9, the shorted potential measurements exhibited some transients after switching. The drop in the potential measured for the gel at 10.0 hours is due to replacing the AE in the reference bath with new AE.

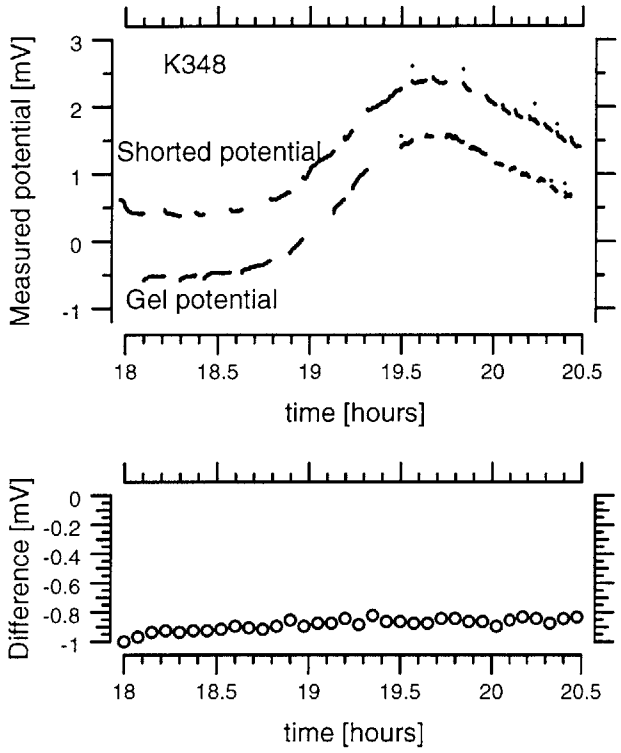

Figure 3-8: The upper graph shows measurements of the three-bath potential as a function of time with K348 in the test bath and AE in the reference bath. The measurements alternate between the gel's potential (the bottom sequence of measurements) and the potential of the two baths shorted (the top measurement sequence). The lower graph shows the corresponding calculated differences between these measured shorted and gel potentials.

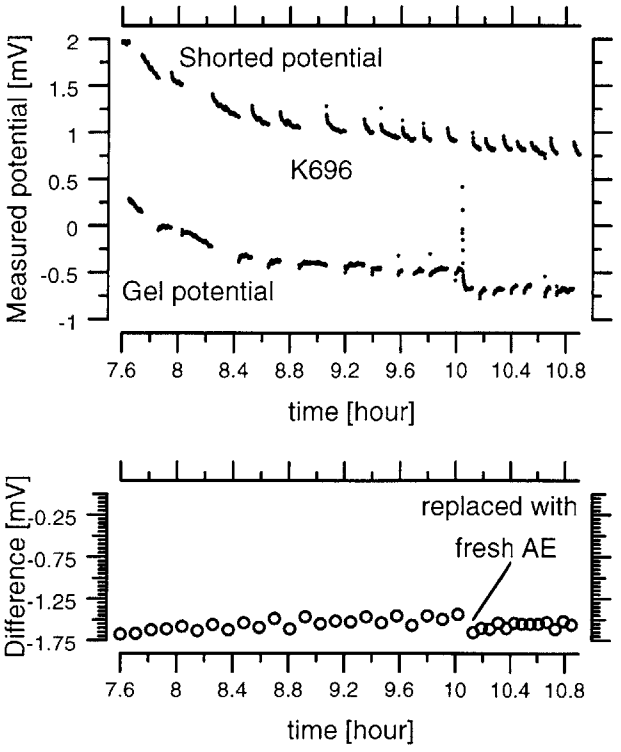

Figure 3-9: Measurements of the three-bath potential as a function of time with the test and reference bath as K696 and AE respectively. The measurements alternate between the gel's potential (the bottom sequence of measurements) and the potential of the two baths shorted (the top measurement sequence). The lower graph shows the corresponding calculated differences between these measured shorted and gel potentials.

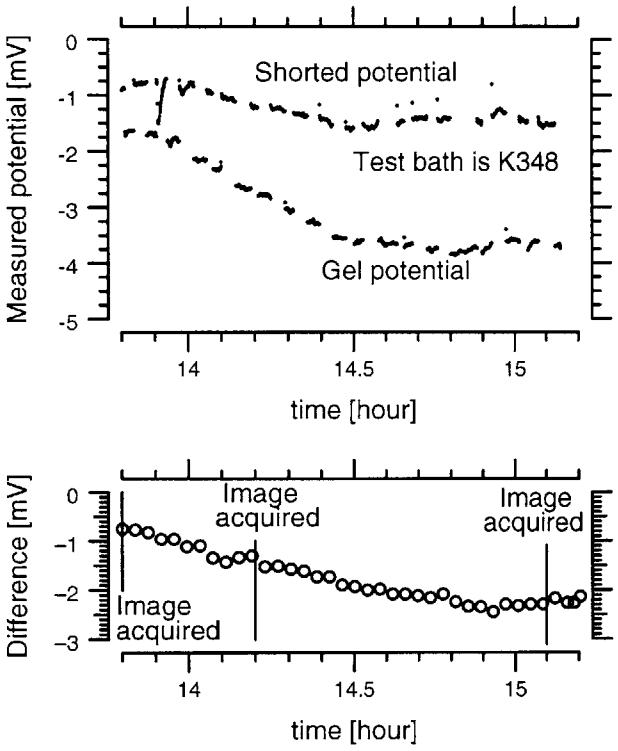

Figure 3-10: Measurement of potential as a function of time using the air-exposed three-bath technique. The test and reference baths were K348 and AE, respectively. The measurements alternate between the gel's potential (the bottom sequence of measurements) and the potential of the two baths shorted (the top measurement sequence). The lower figure shows the corresponding calculated potential differences between these measured shorted and gel potentials.

3.2 Images and potentials measurements of air-exposed gel

Figure 3-10 shows a three-bath experiment where the gel was exposed to air. The test bath was K348 and the reference bath was AE. From 13.8 hours to 15.2 hours, the potential difference changed from -0.75 mV to -2.26 mV.

Figure 3-11 shows images acquired during the same experiment as the potentials shown in figure 3-10. The gel is shown bridging the two edges of the two dishes. From top to bottom, the images were acquired at 13.8 hours, 14.2 hours and 15.1 hours. The gel is noticeably shrinking. The measured voltages corresponding to these images, from top to bottom, were -0.75 mV, -1.5 mV and -2.26 mV.

The air-exposed gel's potential was measured and referenced to the shorted potential for all 4 test baths. All measurements exhibited similar trends. When the gel was initially exposed to air, the potential difference was in the same range as the potential differences measured when the gel was enclosed. Over time the poten-

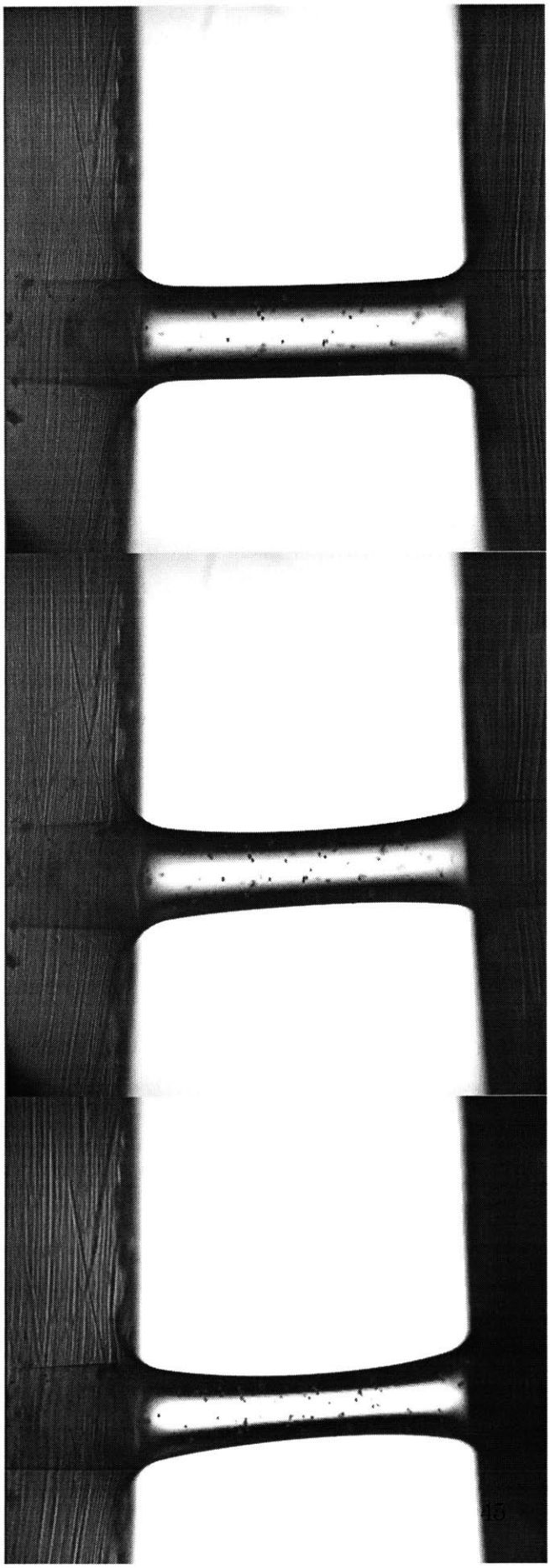

Figure 3-11: Images acquired from an air-exposed two-bath experiment. The gel is shown bridging the edges of two dishes. The reference bath was on the left. The black specks in the gel are flouroscent beads. The images from top to bottom were acquired at 13.8, 14.2 and 15.1 hours. The potential measurements from the same experiment are shown in figure 3-10. The gel is fully hydrated at 13.8 hours and shrunken at 15.1 hours.

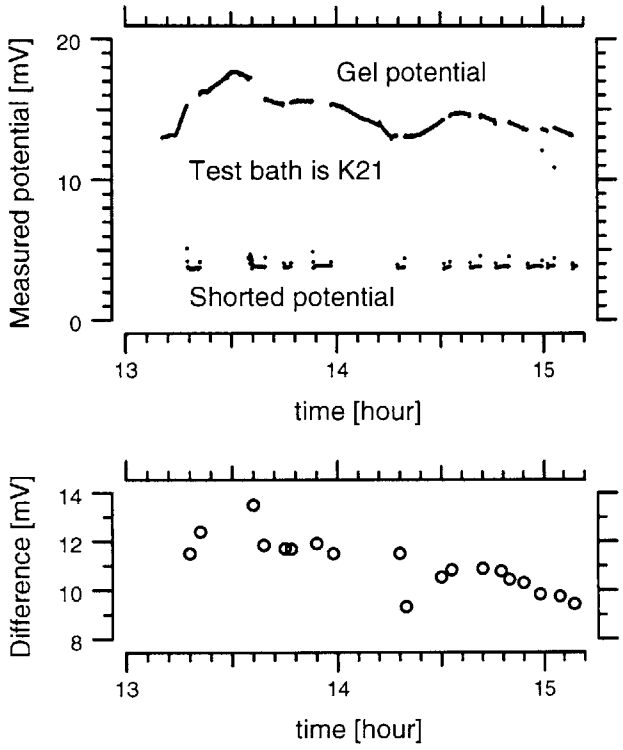

Figure 3-12: Measurement of potential as a function of time using the air-exposed two-bath technique. The test and reference baths were K21 and AE, respectively. The measurements alternate between the gel's potential (the top sequence of measurements) and the potential of the two baths shorted (the bottom measurement sequence). The lower figure shows the corresponding calculated potential differences between these measured shorted and gel potentials.

tial difference would usually increase and sometimes approach a steady state. This potential increase was dependent on the solution in each dish being below a certain amount. Because of the strong capillary forces between the gel and the saline solutions, adjusting the liquid level in the dishes would cause a different length of the gel to be exposed to air. If the maximum possible amount of solution was in each dish, the gel would remain fully hydrated due to capillary action and the potential would not increase. By manually adjusting the solution level, different lengths of the gel were exposed. With enough exposed gel, the potential would begin to increase. This was just observed subjectively, the minimum length of gel needing to be exposed for the potential to increase was not recorded or analyzed.

This correlation between adjustment of the water level and potential can be seen in figure 3-12. The amount of solution in each dish was changed throughout the experiment. However, neither the time of adjustment nor the changing water levels were recorded.

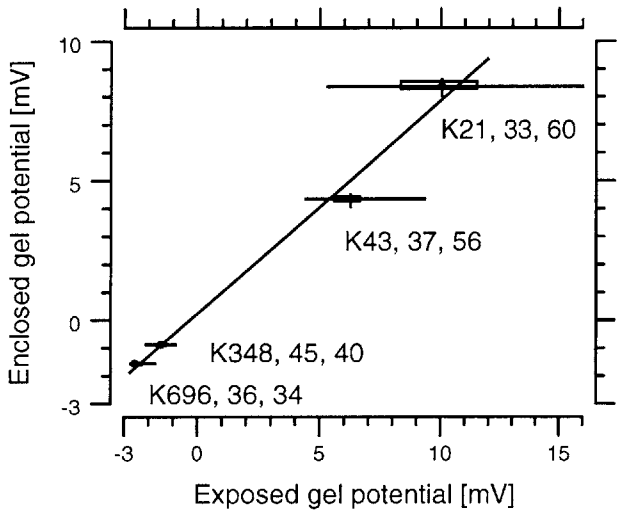

Figure 3-13: Box and whisker plots of enclosed potential measurements (vertical axis) versus air-exposed potential measurements (horizontal axis). Next to each box and whisker plot is the "test bath, number of enclosed potential measurements and number of air-exposed potential measurements at that test bath." The interquartile region is enclosed by a box. The center of the boxes represent the enclosed and air-exposed median measurements. The entire air-exposed and enclosed measurement range at each test bath are spanned with horizontal and vertical lines, respectively.

3.3 Enclosed potentials vs air-exposed potentials

Figure 3-13 shows a double box and whisker plot comparing all the air-exposed measurements with the enclosed measurements. A straight line fit (goodness of fit = 0.995) through the medians has a slope of 0.76 indicating that the air-exposed potential measurements are greater than the enclosed potential measurements. The air-exposed data range at each bath concentration is larger than the data range for the enclosed measurements.

Chapter 4

Analysis of measurements

4.1 Estimating C_f for enclosed measurements

All of the enclosed gel potential measurements after perfusion for the four test baths are combined in a box and whisker plot in figure 4-1. Although the gel potential at each test bath is small, the signal to noise ratio appears to be very good. The voltage range for each is small and there is no overlap in voltage from one concentration to the next. The maximum voltage, 8.5 mV, resulted from the AE-K21 combination. The voltage changes sign when the test bath switched from a concentration less than the reference bath, AE, to a concentration greater than the reference bath.

To see how the DET and the experimental data agree, the boxes and whiskers for the voltage versus test bath are overlaid with curves generated from equation 2.8 in figure 4-2. The data lie between the curves $C_f = -13 \frac{mmol}{L}$ and $C_f = -16.5 \frac{mmol}{L}$. The estimate of fixed charge found by minimizing the square of the difference between the data and equation 2.8 is $C_f = -14.3 \frac{mmol}{L}$ and the DC offset is $V_{DC} =$ 0.209 mV. Figure 4-3 shows the potential measurements with equation 2.13 for $C_f = -14.3 \frac{mmol}{L}$.

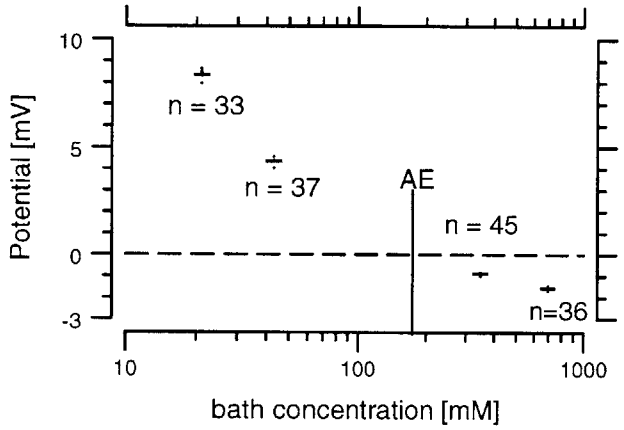

Figure 4-1: Measurements of potential as a function of KCl concentration in the test bath; both baths had a ph $\geq$ 9.5. The reference bath concentration, AE is indicated. The measurements are summarized with whisker plots. The horizontal line indicates the median value. The vertical line indicates the interquartile range. The two vertical dots above and below the vertical line indicate the maximum and minimum data points. The number of experimental data points at each bath concentration is indicated.

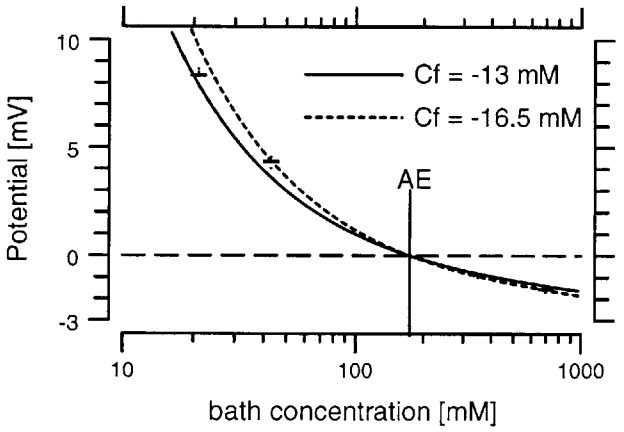

Figure 4-2: The potential measurements of figure 4-1 shown with C_f curves from equation 2.8. The measurements fit between $C_f = -13 \frac{mmol}{L}$ and $C_f = -16.5 \frac{mmol}{L}$. The reference bath concentration, AE is indicated as the test bath concentration where the potential should measure zero.

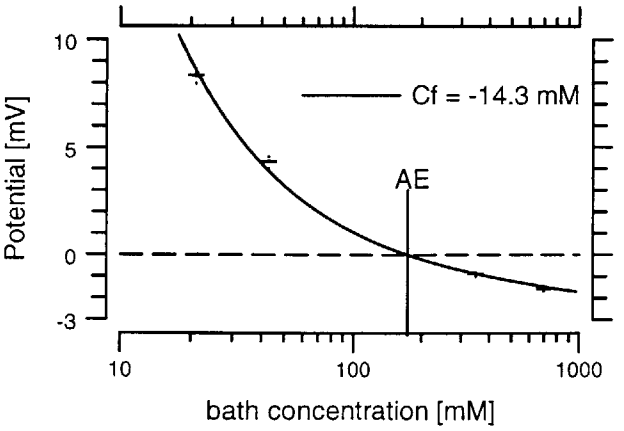

Figure 4-3: The potential measurements of figure 4-1 shown with equation 2.13 evaluated for $C_f = -14.3 \frac{mmol}{L}$. This C_f value minimizes the squared error between equation 2.13 and the potential measurements. The reference bath concentration, AE is indicated as the test bath concentration where the potential should measure zero.

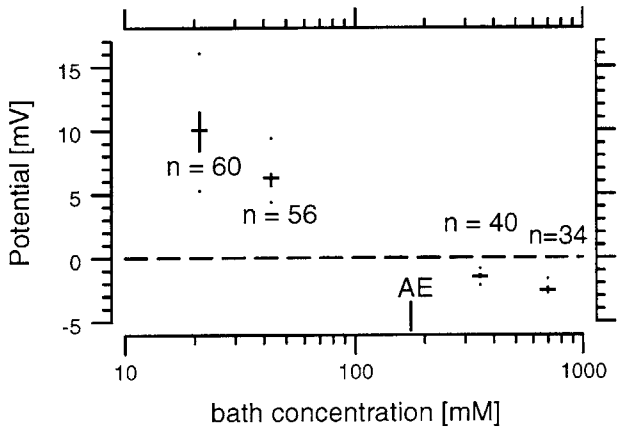

Figure 4-4: Measurements of air-exposed gel potential as a function of KCl concentration in the test bath; both baths had a 9.5≤pH≤10.5. The measurements are summarized with whisker plots that indicate the median and interquartile range. The number of experimental data points at each bath concentration is indicated.

4.2 Estimating C_f for air-exposed measurements

Figure 4-4 shows all of the air-exposed measurements of the gel potential referenced to the short combined into a box and whisker plot. Figure 4-4 shows that when the gel's potential was measured by the air-exposed two-bath technique, there was overlap in the measured potential for K21 and K43 and overlap in the measured potential for K348 and K696. The measured potential was always negative for test bath concentrations greater than the reference bath and always positive for test bath concentrations less than the reference bath.

The boxes and whiskers for the potential versus test bath are overlaid with curves generated from equation 2.13 in figure 4-5. Rather than the data coinciding with one C_f curve; the median measurements lie between the curves $C_f = -17\ \frac{mmol}{L}$ and $C_f = -34\ \frac{mmol}{L}$. The estimate of fixed charge found by minimizing the square of the difference between the data and equation 2.13 is $C_f = -18.8\ \frac{mmol}{L}$. The measurements with equation 2.13 for $C_f = -18.8\ \frac{mmol}{L}$ are shown in figure 4-6.

4.3 Volume changes compared to C_f changes

Figure 4-7 shows a plot of all pairs of air-exposed fixed charge concentration, C_{f_n}, and normalized volume measurements, $\frac{1}{\beta}$, at each test bath concentration.

In figure 4-7, the data, C_{f_n} and $\frac{1}{\beta}$, are approximately proportional. The solid lines through the data for each test bath show the straight-line fit to the data. The

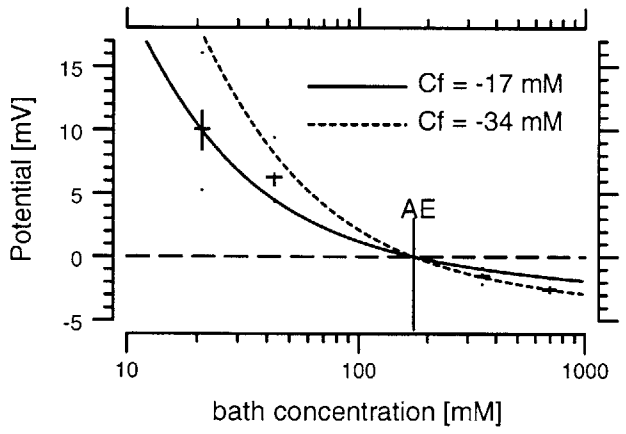

Figure 4-5: The potential measurements of figure 4-4 are shown between equation 2.13 evaluated for $C_f = -17\ \frac{mmol}{L}$ and $C_f = -34\ \frac{mmol}{L}$.

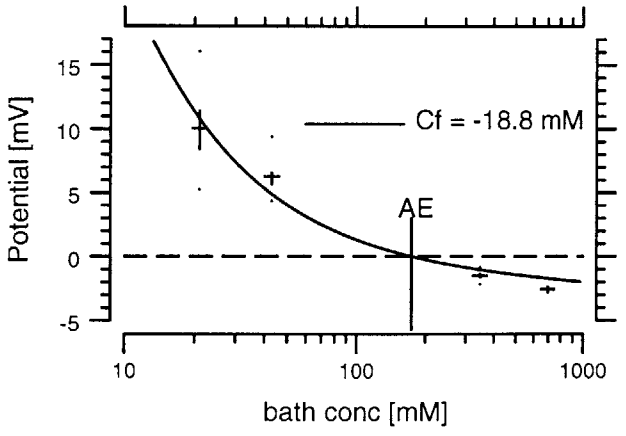

Figure 4-6: The potential measurements of figure 4-4 shown with equation 2.13 evaluated for $C_f = -18.8\ \frac{mmol}{L}$. This C_f value minimizes the squared error between equation 2.13 and the potential measurements.

goodness of the fits for the K21, K43, K348 and K696 data are 0.91, 0.57, 0.74 and 0.81, respectively.

The slope of these lines are $C_{f_o}^{experimental}$. For the test baths K21, K43, K348 and K696, $C_{f_o}^{experimental}$ is 27.6 $\frac{mmol}{L}$, 33.1 $\frac{mmol}{L}$, 35.1 $\frac{mmol}{L}$ and 30.9 $\frac{mmol}{L}$, respectively. The dashed lines shown with the data for each test bath have slopes equal to the median estimated C_f's for the enclosed measurements. For test baths of K21, K43, K348 and K696, the enclosed gel's median estimated C_f is 13.9 $\frac{mmol}{L}$, 16.9 $\frac{mmol}{L}$, 14.7 $\frac{mmol}{L}$ and 15.9 $\frac{mmol}{L}$, respectively. The dashed lines have an intercept of zero. If the dashed line and the data coinicided, that would correspond to a constant number of fixed charges in the gel. In general though, the exposed C_f estimates lay below the dashed line for smaller values of $\frac{1}{\beta}$ and above the dashed line for larger values of $\frac{1}{\beta}$.

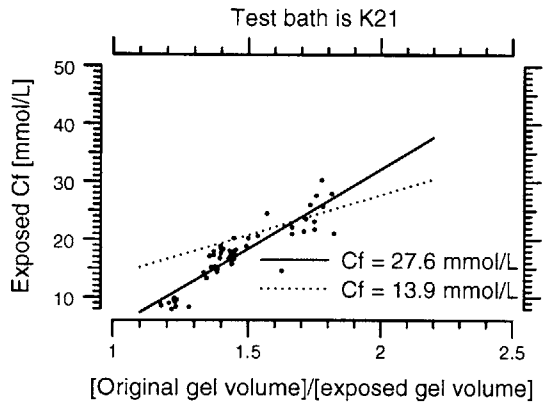

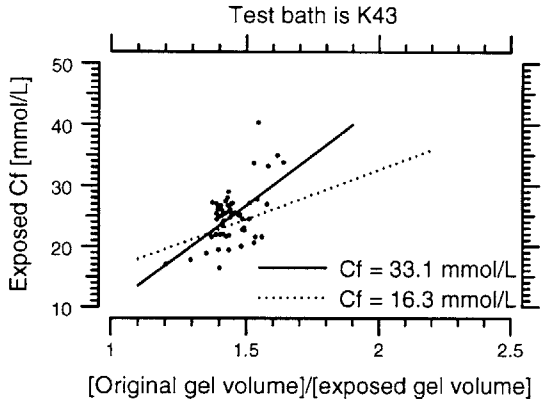

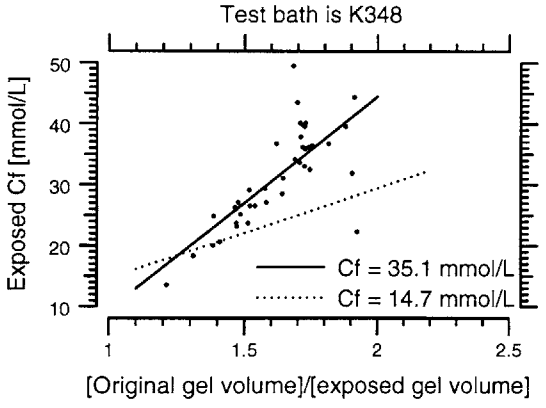

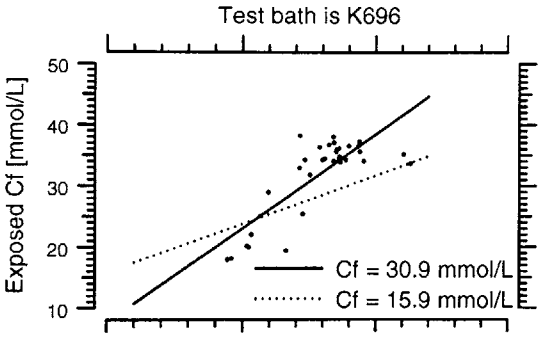

Figure 4-7: Estimated C_f from air-exposed gel potential measurements versus estimated change in gel volume. The results for each test bath are shown separately. In each figure, the solid lines are straight line fits through the data. The slopes of each line are indicated on each figure. Also in each figure, a dashed line is shown with a slope equal to the median estimated C_f for the enclosed measurements. For this line, the intercept is zero.

Chapter 5

Discussion

5.1 Enclosed potential measurements

5.1.1 Stability and variations in enclosed measurements

The gel's absolute potential, without referencing to the shorted two-bath potential, varied unpredictably over time. However, variations were generally slow compared to the measurement time between the gel to short differences. This contributed to the small data range of the results from each test bath. The data range for each test bath was quite small relative to the complete potential range from K21 to K696. From figure 4-1, it can be seen that there was no overlap in potential differences from one test bath to another test bath.

The gel's potential differences acquired with each test bath concentration were repeatable and stable over all experiments. The enclosed gel's potential differences of the potentials would remain constant for over two hours as seen in figure 3-6.

Several experimental methods were employed to stabilize the potential differences and decrease the variations. The measurements were sensitive to the quality of the electrodes. As the age of the electrode increased, the magnitude of the unpredictable variations during an experiment would increase. It was necessary to keep the setup at a constant temperature; if the gel was cooled, the potential difference decreased noticeably.

5.1.2 Perfusion in the enclosed measurements

Perfusing K21 and K43 was essential to eliminating the stagnation layer at the junction between the gel and bath. Measurements of the gel potential when K348 was perfused did not change from measurements of the gel potential when K348 was not perfused. This was true for K696 as well. AE was not perfused for any of the experiments.

5.1.3 Transients in the enclosed measurements

Transients occurred in the gel and shorted potential in the three-bath method but not in the two-bath method. These transients always appeared immediately after switching from gel to short or short to gel measurements. They can be seen in figure 3-9.

One possible cause of the transients was the voltmeter's settling time. During the interval while the shorting bridge was being manually moved from test bath to reference bath, the voltmeter would record an open-circuit voltage around 6 V. Once the shorting bridge was placed back in the fluid, the voltmeter took some time to move back to the smaller potentials.

Another possible cause was an equilibration time. In the three-bath method, the salt gel shorting bridge was alternately placed in the reference bath and the test bath, the salt gel may take some time to equilibrate alternately with the reference bath and the test bath.

5.1.4 DET model and enclosed results

The estimate of C_f was $-14.3\ \frac{mmol}{L}$ which was found by minimizing the difference between the potential measurements and equation 2.13 in a least squared sense. The potential measurements were randomly distributed about the curve generated from equation 2.13 for $C_f = -14.3\ \frac{mmol}{L}$; there were no systematic differences between the measurements and the theory. The median potential measurements fit between $C_f = -13\ \frac{mmol}{L}$ and $C_f = -16.5\ \frac{mmol}{L}$. The data fit the DET model remarkably well

despite many assumptions in the model.

The DET model assumes the gel is in equilibrium with the surrounding ionic bath. However there will be a net ionic flux from the bath with the greater KCl concentration to the bath with the lesser KCl concentration unless there are additional mechanical, osmotic or chemical forces acting on the gel. But the DET model assumes that there are no significant mechanical, chemical or osmotic forces acting on the gel. In the case of K21 and K43 the net ionic flux would be from the reference bath (AE) to the test bath. Since these baths were perfused this flux would not change the concentration of the bath. In the case of K348 and K696, the net ionic flux would be from the test bath to the reference bath. Suggestive of this net ionic flux, figure 3-7, figure 3-8 and figure 3-9 show the potential difference decreasing over time and in the case of figure 3-7 and figure 3-9, when the reference bath was replaced with fresh AE, the potential difference increased.

The two-bath model only considers the junction between the bath and gel. However, a potential could be created within the bulk of the gel. Since K^+ and Cl^- ions are moving through the gel, one potential in the bulk would be the diffusion potential created by the mismatch in mobilities of K^+ ions and Cl^- ions. Another potential would be the streaming potential created by the movement of the mobile ions past the fixed charges. A more accurate model would include potentials within the bulk.

5.2 Air-exposed potential measurements

5.2.1 Stability and variation in potential measurements of air-exposed gel

Similar to the enclosed measurements, the air-exposed gel's potential was referenced to the shorted two-bath potential to eliminate variations not caused by the gel. Similar to the enclosed measurements, these unpredictable variations were generally slow compared to the measurement time between the gel and shorted measurements. The air-exposed gel potential after being referenced to the shorted potential was similar

to the enclosed potential when the experiment began. However, the air-exposed gel's potential difference did not remain similar to the enclosed gel's potential difference.

The air-exposed gel's potential difference was dependent on the length of the gel exposed to air and the amount of time the gel had been exposed to air. As the length of the gel exposed to air increased, the potential difference would increase. The potential difference would also increase as the time that the gel was exposed increased.

5.2.2 Stability and variation in images of air-exposed gel

The images show the gel shrinking. Similar to the potential measurements, the amount of shrinking was dependent on the length of the gel exposed and the amount of time the gel was exposed. The dependence on the length exposed is most clearly illustrated by the fact that if the amount of gel exposed was below a certain length, the gel would not shrink with time. Similar to the potential measurements, the gel would shrink more as the time that the gel was exposed increased.

5.2.3 Changes in gel volume compared to changes in estimated C_f

Figure 4-7 shows the correlation between the estimated C_{f_n} and $\frac{1}{\beta}$, as defined in subsection 2.6.2 and section 2.7. There does appear to be some correlation between the two especially when the test bath was K21, K348 and K696; straight-line fits for these baths have goodness of fits of 0.91, 0.74 and 0.81, respectively.

Besides looking at the straight-line fit to the data, the data were compared to the line with a slope of $C_{f_o}^{enclosed}$ as defined in 2.7. The data tends to fall below the line when the test bath is K21 and to fall above the line for all other test baths. In addition when the data falls below the line, $\frac{1}{\beta}$ is less than 1.5 and when the data falls above the line $\frac{1}{\beta}$ is greater than 1.5.

There was an observed complication that may contribute some understanding on how the geometric changes and estimated C_{f_n} relate to each other. The gel was ex-

tremely hydrophilic. The air-exposed gel between the two baths had solution clinging to it for some distance away from the dish edges. This caused difficulty in determining the exact air-exposed volume to measure. It is also possible there is some concentration of ions in this area that is not equal to the concentration of the ions in the bulk of the baths.

5.3 Conclusion of work

The enclosed gel potential differences fit very well with C_f curves generated from DET. This thesis gives compelling evidence that the fixed charge in a gel can be estimated using the DET model and an enclosed two-bath technique.

The air-exposed measurements had the added variable of exposure to air. Larger potential differences were consistently measured for the air-exposed gel in the two-bath experiments. In addition, the acquired gel images showed the air-exposed gel between the two baths shrinking consistently and simultaneously. The objective was to begin to understand how the gel's geometric changes relate to the changes in the measured potential and hence relate to changes in the estimated C_f.

C_f estimations from the enclosed measurements are likely to be the most reliable results. These results can be used to further understanding of the DET model. Experimental data pairs, $\frac{1}{\beta}$ versus C_{f_n} should lie on a line with a slope equal to $C_{f_o}^{enclosed}$. Since this data does not lie on this line, it appears that this may not be the correct part of the gel of which the DET gives C_f estimations. Based on this data, the DET does not appear to estimate the C_f for the entire piece of gel between the two baths. By analyzing experimental data pairs for different gel volumes, it can be found for which part of the gel, is the C_f estimated.

Bibliography

Abnet, C. C. and Freeman, D. M. (2000). Deformations of the isolated mouse tectorial membrane produced by oscillatory forces, *Hearing Res.* **144**: 29–46.

Allen, J. B. (1980). Cochlear micromechanics – a physical model of transduction, *J. Acoust. Soc. Am.* **68**: 1660–1670.

Davis, H. (1958). A mechano-electrical theory of cochlear action, *Ann. Otol., Rhinol. and Laryngol.* **67**: 789–801.

Freeman, D. M. and Weiss, T. F. (1997). Equilibrium behavior of an isotropic polyelectrolyte gel model of the tectorial membrane, *Auditory Neuroscience* **3**: 351–361.

Ives, D. J. G. and Janz, G. J. (1961). *Reference Electrodes, Theory and Practice*, Academic Press, New York.

Legan, P. K., Lukashkina, V. A., Goodyear, R. J., Kössl, M., Russell, I. J. and Richardson, G. P. (2000). A targeted deletion in α-tectorin reveals that the tectorial membrane is required for the gain and timing of cochlear feedback, *Neuron* **28**: 273–285.

Mammano, F. and Nobili, R. (1993). Biophysics of the cochlea: Linear approximation, *J. Acoust. Soc. Am.* **93**: 3320–3332.

McAllister, A. R. (1998). *Methods of Measuring the Resting Potential of the Tectorial Membrane*, Master of science, Massachusetts Institute of Technology.

McGuirt, W. T., Prasad, S. D., Griffith, A. J., Kunst, H. P. M., Green, G. E., Shpargel, K. B., Runge, C., Huybrechts, C., Mueller, R. E., Lynch, E., King, M. C., Brunner, H. G., Cremers, C. W. R. J., Takanosu, M., Li, S. W., Arita, M., Mayne, R., Prockop, D. J., Camp, G. V. and Smith, R. J. H. (1999). Mutations in *COL11A2* cause non-syndromic hearing loss (DFNA13), *Nature Genet.* **23**: 413–419.

Mitwalli, A. H. (1998). *Polymer Gel Actuator and Sensors*, PhD thesis, Massachusetts Institute of Technology.

Tanaka, T. (1981). Gels, *Sci. Am.* **244**: 124–138.

Verhoeven, K., Laer, L. V., Kirschhofer, K., Legan, P. K., Hughes, D. C., Schatteman, I., Verstreken, M., Hauwe, P. V., Coucke, P., Chen, A., Smith, R. J. H., Somers, T., Offeciers, F. E., Heyning, P. V. D., Richardson, G. P., Wachtler, F., Kimberling, W. J., Willems, P. J., Govaerts, P. J. and Camp, G. V. (1998). Mutations in the human α-tectorin gene cause autosomal dominant non-syndromic hearing impairment, *Nature Gen.* **19**: 60–62.

von Békésy, G. (1947). The variation of phase along the basilar membrane with sinusoidal vibrations, *J. Acoust. Soc. Am.* **19**: 452–460.

von Békésy, G. (1953). Description of some mechanical properties of the organ of Corti, *J. Acoust. Soc. Am.* **25**: 770–785.

Weiss, T. F. (1996). *Cellular Biophysics*, Vol. 1, MIT Press.

Woojin, L. (1996). *Polymer Gel Based Actuator: Dynamic Model of Gel for Real Time Control*, PhD thesis, Massachusetts Institute of Technology.

Zwislocki, J. J. (1979). Tectorial membrane: a possible sharpening effect on the frequency analysis in the cochlea, *Acta Otolaryngol.* **87**: 267–279.

Zwislocki, J. J. and Cefaratti, L. K. (1989). Tectorial membrane II: Stiffness measurements *in vivo*, *Hearing Res.* **42**: 211–228.